Journal of Alloys and Compounds 581 (2013) 530–533

Contents lists available at ScienceDirect

Journal of Alloys and Compounds

journal homepage: www.elsevier.com/locate/jalcom

The strain effect and the ferroelectric field effect in $LaMnO_{3+\delta}$ film/$Pb(Mg_{1/3}Nb_{2/3})O_3$–$PbTiO_3$ single-crystal heterostructures

Q.X. Zhu [a], M.M. Yang [a], M. Zheng [a], W. Wang [a], Y. Wang [c], X.M. Li [a,*], H.S. Luo [a], X.G. Li [b], H.L.W. Chan [c], R.K. Zheng [a,*]

[a] State Key Laboratory of High Performance Ceramics and Superfine Microstructure, Shanghai Institute of Ceramics, Chinese Academy of Sciences, Shanghai 200050, China
[b] Hefei National Laboratory for Physical Sciences at Microscale and Department of Physics, University of Science and Technology of China, Hefei 230026, China
[c] Department of Applied Physics and Materials Research Center, The Hong Kong Polytechnic University, Hong Kong, China

ARTICLE INFO

Article history:
Received 15 May 2013
Received in revised form 6 June 2013
Accepted 10 July 2013
Available online 18 July 2013

Keywords:
Strain effect
Ferroelectric field effect
Manganite film
PMN–PT crystal

ABSTRACT

The evolution of the competition and coaction between the ferroelectric field effect and the strain effect with temperature has been studied for the $LaMnO_{3+\delta}$ film/$Pb(Mg_{1/3}Nb_{2/3})O_3$–$PbTiO_3$ crystal heterostructure. The polarization-rotation-induced strain has a dramatic impact on the electronic transport properties at room temperature. Upon cooling, the polarization-rotation-induced interfacial charge effect competes with and finally overwhelms the strain effect, and modulates the transport and magnetic properties of the $LaMnO_{3+\delta}$ film reversibly via the depletion or accumulation of hole carriers at interface. The identification of charge carrier-mediated electric-field-control of the electronic transport and magnetic properties would help researchers better understand the magnetoelectric coupling mechanism in manganite film/ferroelectric crystal heterostructures.

1. Introduction

Magnetoelectric heterostructures composed of ferromagnetic (FM) thin films epitaxially grown on ferroelectric (FE) single-crystal substrates have received great attention in the past decade due to their rich fundamental physics and potential applications in future multifunctional devices [1–3]. For such unique heterostructures, not only the substrate clamping effect but also the leakage current caused by the FE layer in this artificially-assembled structures could be completely avoided, thereby maximizing the in-plane elastic strain coupling at interface and giving rise to a larger strain-mediated magnetoelectric effect [4]. Hole doped manganites $R_{1-x}A_xMnO_3$ (R = La, Pr, etc., A = Ca, Sr, or Ba) have been epitaxially grown on FE substrates, e.g. $BaTiO_3$ and $Pb(Mg_{1/3}Nb_{2/3})O_3$–$PbTiO_3$ (PMN–PT), to form "FM film/FE crystal" heterostructures whose electronic transport, magnetic, and magnetoelectric effect attracted tremendous studies [3,5–8]. For such $R_{1-x}A_xMnO_3$ film/FE crystal heterostructures, it is generally believed that the electric-field-induced modulation of the spin and charge degrees of freedom is microscopically due to the elastic strain coupling at interface [3,9,10], whereas the electric-field-induced accumulation or depletion of electric charges at interface (i.e., the ferroelectric field effect) is usually ignored for these heterostructures. Electric-field modulation of charge carrier density in perovskite manganite films has been achieved by employing ferroelectric thin film (e.g., $PbZr_{0.52}Ti_{0.48}O_3$) as gate materials [11,12]. It is known that perovskite manganites are spin, charge, lattice, and orbital degrees of freedom strongly correlated material systems whose phase diagrams are critically dependent on the carrier density [13,14]. Consequently, both the electric-field-induced lattice strain effect and the ferroelectric field effect would have great impact on the physical properties of manganite thin films, which has recently been observed in the $Pr_{0.5}Ca_{0.5}MnO_3$/$0.67Pb(Mg_{1/3}Nb_{2/3})O_3$-$0.33PbTiO_3$ heterostructures [15].

The parent compound of doped lanthanum manganites, $LaMnO_3$, is an insulating material which shows cooperative Jahn–Teller (JT) distortion of MnO_6 octahedra, $d_{3x^2-r^2}/d_{3y^2-r^2}$ orbital order, and *A*-type antiferromagnetic spin ordering [16]. $LaMnO_3$ compound usually exhibits oxygen nonstoichiometry [17–19], as reflected in the general formula of $LaMnO_{3+\delta}$ ($\delta \geqslant 0$) (LMO). The excess of oxygen causes a portion of Mn^{3+} ions to be oxided to Mn^{4+} ions, making LMO compounds have similar physical behaviors as lightly hole doped lanthanum manganites [20]. In this study, we epitaxially grow the LMO film on polished ferroelectric PMN–PT single-crystal substrate ($a \sim b \sim c \sim 4.02$ Å) that displays excellent ferroelectric and piezoelectric activities [21] and experimentally demonstrate the coaction and competition between the ferroelectric field effect and the strain effect, as illustrated by a remarkable temperature dependent electric-field-manipulation of the electronic transport and magnetic properties.

* Corresponding authors. Tel.: +86 21 52411205.
E-mail addresses: lixm@mail.sic.ac.cn (X.M. Li), zrk@ustc.edu (R.K. Zheng).

0925-8388/$ - see front matter © 2013 Elsevier B.V. All rights reserved.
http://dx.doi.org/10.1016/j.jallcom.2013.07.061

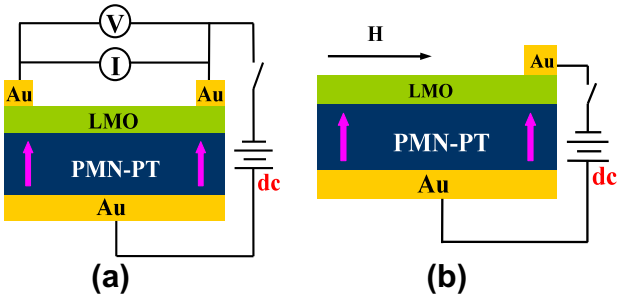

Fig. 1. Schematic diagrams of the LMO/PMN–PT structure and the electrical configuration for measurements of the resistance (a) and the magnetization (b). The arrow in the PMN–PT represents the poling direction.

2. Experimental details

LMO films were deposited on one-side-polished and ⟨001⟩-oriented PMN–PT single-crystal substrates using dc magnetron sputtering [19]. The deposition was carried out in an argon–oxygen flow with 60% Ar and 40% O_2 at a pressure of 5 Pa and a substrate temperature of 700 °C. After deposition, the films were *in situ* cooled to room temperature and postannealed in air at 700 °C for 30 min using a rapid thermal processor furnace. The thickness of films was measured to be ~30 nm using a JSM-6700F scanning electron microscope. The surface morphology of films was obtained using an atomic force microscope (Nanocute SII, Seiko, Japan). The phase purity and epitaxial quality of the film were investigated by X-ray diffraction (XRD) θ–2θ scan and ϕ-scan, respectively, using a high resolution four-circle Bruker D8 Discover X-ray diffractometer equipped with a 4-bounce Ge(220) monochromator and Cu Kα_1 radiation. Transport and magnetic properties of LMO films were measured using a Physical Property Measurement System (PPMS-9, Quantum Design) and a SQUID magnetometer (MPMS-XL5, Quantum Design), respectively. The measurement circuits are illustrated in Fig. 1(a and b), respectively. A strain gauge was bonded to the PMN–PT using epoxy in order to analyze the strain versus electric field loop of the PMN–PT substrate.

3. Results and discussion

The LMO film is single phase and *c*-axis oriented as checked by XRD θ–2θ scan (Fig. 2(a)). Both the PMN–PT and the LMO bulk materials hold a pseudocubic unit cell with lattice parameters $a \sim b \sim c \sim 4.02$ Å for the former and $a \sim b \sim c \sim 3.91$ Å for the latter. In spite of the relative large lattice mismatch between the LMO compound and the PMN–PT crystal, the LMO film still grows epitaxially on the PMN–PT crystal, indicated by the XRD ϕ-scan patterns of the LMO (101) and PMN–PT (101) planes (Fig. 2(b)). The *c*- and *a*-axis lattice constants of the LMO film are calculated to be ~3.887 Å and ~3.95 Å ($c/a < 1$), respectively, indicating that the film is subjected to out-of-plane compressive and in-plane tensile strain. Fig. 2(d) shows the surface morphology of the LMO film with a root-mean-square roughness (R_{rms}) of ~1 nm. The PMN–PT substrate exhibits excellent ferroelectric and piezoelectric properties, which is evidenced by a typical rectangular like ferroelectric polarization versus electric field (*P*–*E*) loop and a well-defined butterfly like strain versus electric field (ε-*E*) loop (Fig. 2(c)). Note that the *P*–*E* loop is antisymmetric while the ε-*E* loop is symmetric with respect to the sign of the applied electric field. The fundamentally different shape between the *P*–*E* loop and the ε-*E* loop can be used to distinguish which effect (i.e., the ferroelectric field effect or the strain effect) exerts major influence on the modulation of physical properties of LMO film.

Fig. 3 shows the temperature dependence of the resistance for the LMO film when the PMN–PT substrate was in different polarized states. For unpolarized state, the resistance of the LMO film increases with decreasing temperature from 300 K and undergoes an insulator-to-metal like transition at $T_P = 171$ K. With further decrease in the temperature, the resistance shows a rapid upturn, which is probably due to the formation of charge-ordered (CO)

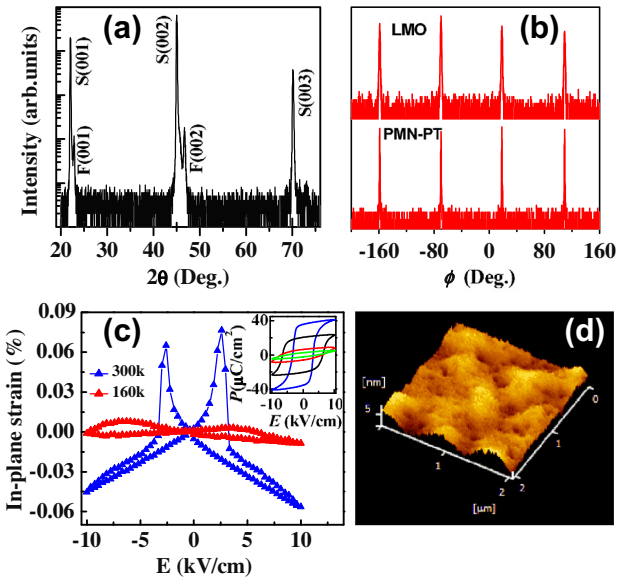

Fig. 2. (a) X-ray diffraction pattern for the LMO/PMN–PT structure. The "S" and "F" stand for substrate and film, respectively. (b) XRD phi scans taken on the LMO (101) and PMN–PT (101) diffraction peaks, (c) in-plane piezo-strain versus *E* curve for the PMN–PT substrate at $T = 300$, 160 K. The inset shows the *P*–*E* hysteresis loop for the PMN–PT substrate at $T = 300$ K (the blue one), 210 K (the black one), 180 K (the red one), and 160 K (the green one), respectively and (d) The surface morphology of the LMO film. (For interpretation of the references to colour in this figure legend, the reader is referred to the web version of this article.)

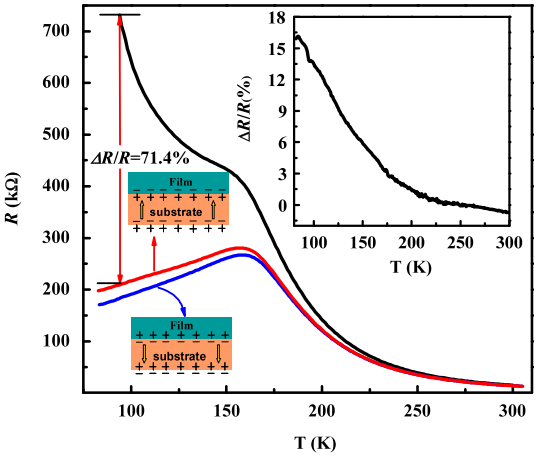

Fig. 3. Temperature dependence of the resistance for the LMO film when the PMN–PT substrate was in different polarized states. The inset shows the relative change in the resistance of the LMO film with the polarization state changing from P_r^- to P_r^+, $\Delta R/R$ is defined as $\Delta R/R = [R(P_r^+) - R(P_r^-)]/R(P_r^-)$.

phase [18,22], in which mobile e_g electrons become localized and ordered. After the measurements of the resistance as a function of temperature when the PMN–PT substrate was in the unpolarized state, a dc poling field of +10 kV/cm was applied to the LMO/PMN–PT structure through the top and bottom electrodes at $T = 296$ K so that the PMN–PT substrate was poled to positively polarized state (i.e., the polarization direction points to the LMO film, referred to as P_r^+ state), as schematically indicated by the arrows in Fig. 3. After the PMN–PT substrate had been poled to P_r^+ state, the +10 kV/cm poling field was turned off. Since the ferroelectric Curie temperature (~155 °C) of the PMN–PT substrate is much higher than room temperature, the polarization direction